Spectral and Kinetic Studies of the Oxidation of Monosubstituted Phenols and Anilines by Recombinant *Synechocystis* Catalase−Peroxidase Compound I[†]

Günther Regelsberger,[‡] Christa Jakopitsch,[§] Markus Engleder,[‡] Florian Rüker,[||] Günter A. Peschek,[§] and Christian Obinger*[,‡]

Institute of Chemistry, University of Agricultural Sciences, Muthgasse 18, A-1190 Vienna, Institute of Physical Chemistry, University of Vienna, Althanstrasse 14, A-1090 Vienna, and Institute of Applied Microbiology, University of Agricultural Sciences, Muthgasse 18, A-1190 Vienna, Austria

Received April 15, 1999; Revised Manuscript Received June 28, 1999

ABSTRACT: A high-level expression in *Escherichia coli* of a fully active recombinant form of a catalase−peroxidase (KatG) from the cyanobacterium *Synechocystis* PCC 6803 is reported. Since both physical and kinetic characterization revealed its identity with the wild-type protein, the large quantities of recombinant KatG allowed the first examination of second-order rate constants for the oxidation of a series of aromatic donor molecules (monosubstituted phenols and anilines) by a bifunctional catalase−peroxidase compound I using the sequential-mixing stopped-flow technique. Because of the overwhelming catalase activity, peroxoacetic acid has been used for compound I formation. A ≥50-fold excess of peroxoacetic acid is required to obtain a spectrum of relatively pure and stable compound I which is characterized by about 40% hypochromicity, a Soret maximum at 406 nm, and isosbestic points between the native enzyme and compound I at 357 and 430 nm. The apparent second-order rate constant for formation of compound I from ferric enzyme and peroxoacetic acid is $(8.74 \pm 0.26) \times 10^3$ M^{-1} s^{-1} at pH 7.0. Reduction of compound I by aromatic donor molecules is dependent upon the substituent effect on the benzene ring. The apparent second-order rate constants varied from $(3.6 \pm 0.1) \times 10^6$ M^{-1} s^{-1} for *p*-hydroxyaniline to $(5.0 \pm 0.1) \times 10^2$ M^{-1} s^{-1} for *p*-hydroxybenzenesulfonic acid. They are shown to correlate with the substituent constants in the Hammett equation, which suggests that in bifunctional catalase−peroxidases the aromatic donor molecule donates an electron to compound I and loses a proton simultaneously. The value of ρ, the susceptibility factor in the Hammett equation, is -3.4 ± 0.4 for the phenols and -5.1 ± 0.8 for the anilines. The pH dependence of compound I reduction by aniline exhibits a relatively sharp maximum at pH 5. The redox intermediate formed upon reduction of compound I has spectral features which indicate that the single oxidizing equivalent in KatG compound II is contained on an amino acid which is not electronically coupled to the heme.

On the basis of sequence similarities with fungal cytochrome *c* peroxidase (CCP) and plant ascorbate peroxidases (APX), bacterial catalase−peroxidases (KatG) have been shown to be members of class I of the superfamily of plant, fungal, and bacterial peroxidases (*1*). The enzymes from plants and fungi are monomeric or homodimeric and have subunits with a size of 290−350 amino acid residues, whereas subunits in homodimeric or tetrameric bacterial catalase−peroxidases are double in length, adding up to about 80−85 kDa, which is ascribed to gene duplication (*2*). Each half of a KatG monomer is homologous to CCP or APX, but the N-terminal half is more closely related and most probably contains the heme-binding site (*2*). From both CCP and APX, the three-dimensional structures are known (*3*, *4*) and exhibit highly conserved amino acid residues at the active site. Unfortunately, no structural data are available from catalase−peroxidases, but both physical characterizations and sequence analyses (*5*−*10*) unequivocally suggest the presence of histidine as the proximal ligand. As with APX and CCP, the proximal histidine seems to have an imidazolate character because its δ-nitrogen seems to be H-bonded to a conserved aspartate residue. In APX and CCP, the latter is H-bonded to a tryptophan residue which is also conserved in KatG proteins. The high-resolution crystal structures of both CCP and APX indicate the presence of the triad Arg-Trp-His at the distal side as well as a H-bond from the δ-nitrogen of the distal His to a near-surface asparagine. Sequence alignments suggest the presence of these residues also in the distal pocket of catalase−peroxidases. Though there are these striking similarities regarding the active site, the catalytic activity and substrate specificity of these three peroxidase species are completely different. The most interesting feature of bifunctional catalase−peroxidases is the overwhelming catalase activity with k_{cat}/K_m values comparable with those of monofunctional catalases. Interestingly, the catalase activity of the homologous members of class I, CCP and APX, is very small, and at the moment,

[†] This work was supported by the Austrian Science Foundation (FWF-Project P12371-MOB).

* To whom correspondence should be addressed: Institute of Chemistry, University of Agricultural Sciences, Muthgasse 18, A-1190 Vienna, Austria. Telephone: +43-1-36006-6073. Fax: +43-1-36006-6059. E-mail: cobinger@edv2.boku.ac.at.

[‡] Institute of Chemistry, University of Agricultural Sciences.

[§] Institute of Physical Chemistry, University of Vienna.

[||] Institute of Applied Microbiology, University of Agricultural Sciences.

10.1021/bi990886n CCC: $18.00
Published on Web 07/21/1999

there seems to be no structural basis for understanding these striking differences. In addition to their catalase activities, catalase−peroxidases function as broad specificity peroxidases, oxidizing various electron donors, including NAD(P)H (*6*, *9*, *10*), guaiacol (*8*), pyrogallol (*6*−*10*), and *o*-dianisidine (*6*−*10*) with both the ratio of catalase to peroxidase activity and donor specifity varying among different members of this peroxidase type. On the contrary, typical electron donors for CCP and APX, cytochrome *c* and ascorbate, respectively, have been demonstrated to be extremely poor electron donors for KatG enzymes (*11*).

In the meanwhile, catalase−peroxidases have been isolated and characterized from a variety of different bacteria, including *Escherichia coli* (*12*), *Bacillus stearothermophilus* (*13*), *Klebsiella pneumoniae* (*14*), *Rhodobacter capsulatus* (*15*, *16*), *Streptomyces* sp. (*5*), *Mycobacterium smegmatis* (*6*), and *Mycobacterium tuberculosis* (*9*, *10*). Finally, KatG has been shown to be the only hydrogen peroxide-scavenging enzyme in the cyanobacteria *Synechococcus* PCC 7942 (*7*), *Synechococcus* PCC 6301 (*17*), and *Synechocystis* PCC 6803 (*8*). Though the overexpression of KatG from several species has been reported (*7*, *9*, *10*, *13*, *16*), so far no detailed studies on kinetic and spectroscopic properties of KatG redox intermediates have been reported.

Here we describe a system for the expression of large quantities of fully active recombinant catalase−peroxidase from the cyanobacterium *Synechocystis* PCC 6803 and demonstrate its suitability for transient-state kinetic investigations. We, for the first time, report the spectral characteristics of KatG compounds I and II and the rates of reaction of 11 aromatic donor molecules with *Synechocystis* KatG compound I determined by sequential-mixing stopped-flow spectroscopy. With aniline, the pH-dependent rate profile is obtained. The results are correlated using the Hammett $\rho\sigma$ relation (*18*). A mechanism for KatG compound I reduction by aromatic one-electron donors is suggested.

EXPERIMENTAL PROCEDURES

Materials. Materials were obtained from the following sources: bovine serum albumin (BSA), human angiotensin I, bee venom melittin, sinapinic acid, α-cyano-4-hydroxycinnamic acid, trypsin, peroxoacetic acid, hydrogen peroxide, and ascorbic acid from Sigma; *p*-hydroxyaniline, *p*-toluidine, *m*-aminobenzoic acid, *m*-aminoacetophenone, sulfanilic acid, *p*-hydroxyanisole, *m*-hydroxyanisole, *p*-hydroxybenzenesulfonic acid, and *p*-chlorophenol from Aldrich; the QIAEX II Gel Extraction Kit from Qiagen; Chelating Sepharose Fast Flow and HiPrep Sephacryl S-300 HR 16/60 columns from Amersham Pharmacia Biotech; the Centriprep-30 concentrators from Amicon; *Nde*I, *Bam*HI, and *Bgl*II restriction enzymes, alkaline phosphatase, and DNA ligase from Boehringer Mannheim; ex-Taq DNA polymerase from TaKaRa; and $K_4[Fe(CN)_6]$, aniline, and phenol from Merck. All other reagents were of highest grade available.

Growth Conditions and Overexpression. *Synechocystis* PCC 6803 was grown in BG-11 medium (*19*) at 35 °C for 1 week under illumination and bubbling with 1% (v/v) CO_2 in sterile air, and the chromosomal DNA was isolated (*20*). Synthetic oligonucleotide primers were purchased from Codon GmbH (Weiden a. S., Austria). Primer 1 (5′-GGG AAT TCC ATA TGG GCA CCC AAC CCG CCA G-3′) consisted of 31 bases with a ATG start codon and an *Nde*I restriction site, and primer 2 (5′-GGA AGA TCT CTA ATG GTG GTG ATG GTG GTG GCC CCT AGG GAG ATC AAA CCG-3′) consisted of 51 bases with a TAG termination codon, a sequence coding for a hexahistidine tag, and a *Bgl*II restriction site. These primers, the chromosomal DNA from *Synechocystis* as the template, and the ex-Taq polymerase were used for PCR under the following conditions: 94 °C for 2 min (hot start); 28 cycles at 92 °C for 40 s, 47 °C for 1 min, and 72 °C for 3 min; and finally at 72 °C for 10 min. The PCR products were fractionated on a 1% agarose gel, and the appropriate DNA was cut out and purified using the QIAEX II Gel Extraction Kit. This DNA fragment was digested with restriction enzymes *Nde*I and *Bgl*II and cloned into the *Nde*I- and *Bam*HI-digested, alkaline phosphatase-treated expression vector pET-3a (*21*). The insert was sequenced by the dideoxy chain termination method (*22*) using an Applied Biosystems 373A DNA sequencer.

Competent *E. coli* BL21(DE3)pLysS cells were transformed with the expression vector by electroporation (Gene Pulser, Bio-Rad, Hercules, CA), and positive clones carrying the recombinant plasmid were selected and grown overnight on an orbital shaker (180 rpm) at 37 °C in LB medium containing 100 μg/mL ampicillin and 25 μg/mL chloramphenicol. After dilution of the cell suspension with M9ZB medium containing the same antibiotics, the culture was cooled to 16 °C and expression of catalase−peroxidase was induced by the addition of 1 mM isopropyl β-D-thiogalactopyranoside (IPTG). At the time of induction, hemin was added to a final concentration of 40 μg of hemin/mL of medium. After incubation for 4 h at 16 °C, cells were harvested by centrifugation (18000*g* for 20 min at 4 °C) and resuspended in lysis buffer [50 mM Tris/HCl (pH 8.0) containing 2 mM EDTA and 0.1% Triton X-100]. Phenylmethanesulfonyl fluoride (1 mM), leupeptin (5 μM), and pepstatin (5 μM) were added, and the cells were broken by three cycles of freezing and thawing and sonication with short bursts. The suspension was centrifuged (21000*g* for 20 min at 4 °C), and from the supernatant, KatG was purified.

Protein Purification. The supernatant was adjusted to 1 M NaCl and 20 mM imidazole and loaded on a Chelating Sepharose Fast Flow column (1.6 cm × 10 cm) charged with 30 μmol of Zn^{2+}/mL of gel and equilibrated with 67 mM phosphate buffer (pH 7.0) containing 1 M NaCl and 20 mM imidazole at 4 °C. The column was washed with 200 mL of the equilibration buffer, and bound proteins were eluted with 100 mL of a gradient of 20 to 500 mM imidazole in 67 mM phosphate buffer (pH 7.0) containing 1 M NaCl. The eluted proteins were concentrated, and the buffer was exchanged with Centriprep concentrators. Proteins were loaded onto a Sephacryl column equilibrated with 67 mM phosphate buffer (pH 7.0) containing 150 mM KCl, at room temperature. Active fractions were concentrated using Centriprep concentrators.

For molecular weight determination, the column was calibrated with a mixture of low- and high-molecular mass standards (Pharmacia) in the range of 13.7−669 kDa.

Electrophoresis. SDS−PAGE was carried out on 12% slab gels as described by Laemmli (*23*) using SigmaMarkers and the Bio-Rad Mini-Protean II system. Proteins on the gel were stained with Coomassie Blue.

Activity Assays. The concentration of the enzyme solution was determined spectrophotometrically with an ϵ_{406} of 1.02 $\times$ 10^5 M^{-1} cm^{-1} per heme (*17*). Catalase activity was determined with 5 mM H_2O_2 in 67 mM phosphate buffer (pH 7.0) either polarographically using a Clark-type electrode (YSI 5331 Oxygen Probe) inserted into a stirred water bath (YSI 5301B) at 30 °C or spectrophotometrically (*24*) using an extinction coefficient for hydrogen peroxide at 240 nm of 39.4 M^{-1} cm^{-1} (*25*) at 25 °C. Peroxidase activity was monitored spectrophotometrically using 1 mM H_2O_2 and 1 mM *o*-dianisidine by following the oxidation rate at 460 nm (ϵ_{460} = 11.3 mM^{-1} cm^{-1}) at 25 °C in 67 mM phosphate buffer (pH 7.0).

Peptide Mass Mapping. MALDI-TOF-MS (matrix-assisted laser desorption ionization time-of-flight mass spectrometry) was carried out on a DYNAMO MALDI-TOF-MS system (Thermo BioAnalysis, Santa Fe, NM) in the dynamic extraction mode (setting 0.1). For determining the accurate mass of the protein, sinapinic acid was used as the matrix and external calibration was performed using bovine serum albumin. For peptide mass mapping, the catalase−peroxidase was loaded onto an SDS gel, stained with Coomassie Blue, and digested as described by Jensen et al. (*26*). The peptide masses after tryptic digestion were compared with calculated peptide masses using the PeptideMass software (*27*). The software is freely available via the ExPASy World Wide Web server, at the URL address http://www.expasy.ch/www/tools.html. The protein sequence of the catalase−peroxidase was obtained from the CyanoBase, the genome database for *Synechocystis* PCC 6803, at http://www.kazusa.or.jp/cyano/cyano.orig.html (*28*). The protein and peptide samples were mixed with a 1% solution of the matrix in 70% acetonitrile. One microliter of these mixtures was deposited to a probe, air-dried, and inserted into the mass spectrometer to acquire a spectrum.

Transient-State Experiments. All transient-state measurements were performed in 50 mM phosphate buffer (pH 7.0) with the exception of pH dependence studies on reaction rates for which the experimental traces were recorded in 50 mM citrate/phosphate buffers at different pH values between 4.0 and 8.0.

Stopped-flow experiments were performed using an Applied Photophysics instrument (model SX-18MV) equipped with a 1 cm observation cell thermostated at 15 °C. Rate constants from experimental traces were calculated by the SpectraKinetic Workstation v4.38 interfaced with the apparatus. Sequential stopped-flow analysis was used to investigate the reduction of compound I because it is inherently unstable. To form compound I, 4 μM enzyme was mixed with 200 μM peroxoacetic acid in the aging loop. Twenty seconds after the initial mixing, compound I was allowed to react with various concentrations of one-electron substrates. In the observation cell, the final concentrations were 1 μM for the enzyme and 50 μM for the peroxide. At least three determinations of the pseudo-first-order rate constants, k_{obs}, were measured for each substrate concentration, and the mean value was used to calculate the second-order rate constants. To allow calculation of pseudo-first-order rates, the concentrations of substrates were at least 5 times higher than that of the enzyme. The slope of the linear plot of the pseudo-first-order rate constant versus substrate concentration was used to obtain the second-order rate constant for the reaction. For determining the pH dependence of rate constants for compound I reduction, the pH jump technique was used. Compound I was formed by mixing enzyme and peroxoacetic acid at pH 7.0 in 5 mM phosphate buffer. After a delay time of 20 s, compound I reacted with substrate in 100 mM citrate/phosphate buffer (pH 4.0−8.0) to give a final buffer concentration of 50 mM.

Rapid-scan absorption spectra were recorded by means of a photodiode array detector and the XScan Diode Array Scanning v1.07 software. The spectral region of 200−700 nm was scanned by measuring 400 spectra within 2 s. Compound I was formed by mixing 80 μM enzyme with 800 μM peroxoacetic acid in the aging loop. Twenty seconds after the initial mixing, compound I was allowed to react with one-electron substrates such as anilines, phenols, ascorbic acid, or $K_4[Fe(CN)_6]$. In the observation cell, the final concentrations were 20 μM for the enzyme and 200 μM for the peroxide. For recording the spectrum of native catalase−peroxidase, the one-electron substrate and peroxide solutions were replaced with water; and for recording the spectrum of compound I, the one-electron substrate solution was replaced with water.

The rate of reduction of compound I was also measured on a time scale of seconds using a Zeiss Specord S-10 diode array spectrophotometer. In a 1 mL cuvette, 20 μM catalase−peroxidase was incubated with 1 mM peroxoacetic acid for 20 s to form compound I and then reduced with anilines, phenols, ascorbate, or $K_4[Fe(CN)_6]$.

RESULTS

Expression in E. coli and Purity of the Recombinant Enzyme. Recently, we have purified a catalase−peroxidase from *Synechocystis* PCC 6803 encoded by the *katG* gene (*8*). The *katG* gene has a 2262 bp open reading frame, encoding a catalase−peroxidase (KatG) of 754 amino acid residues (*8*). Here, we have extended its entire coding DNA using a synthetic oligonucleotide encoding a hexahistidine tag at the C-terminus and expressed it in *E. coli* [BL21(DE3)-pLysS] using the pET-3a vector. Addition of hemin was necessary to ensure its proper association with KatG upon induction. A 1 L culture of *E. coli* yielded between 30 and 40 mg of active protein. The expressed protein was purified to homogeneity by two chromatography steps, including metal chelate affinity and gel filtration chromatography. During metal chelate affinity chromatography, almost all *E. coli* proteins, including host catalase activity, eluted at the washing step. As a control, *E. coli* cells were transformed with the pET vector containing no catalase−peroxidase insert and cell lysate was loaded on the affinity column. After the column had been washed, no catalase activity was detected in fractions eluted with an imidazole gradient. In total, the purification procedure had a final recovery between 23 and 31% of catalase activity.

Purified KatG ran as a single band of approximately 85 kDa on SDS−PAGE (not shown), whereas with gel filtration chromatography, a value of approximately 170 kDa was obtained (not shown), suggesting a homodimeric form of the enzyme, which is in full agreement with the physical properties of the wild-type enzyme (*8*). To underline these findings, the molecular mass of recombinant KatG was also determined by MALDI-TOF, exhibiting a single peak at

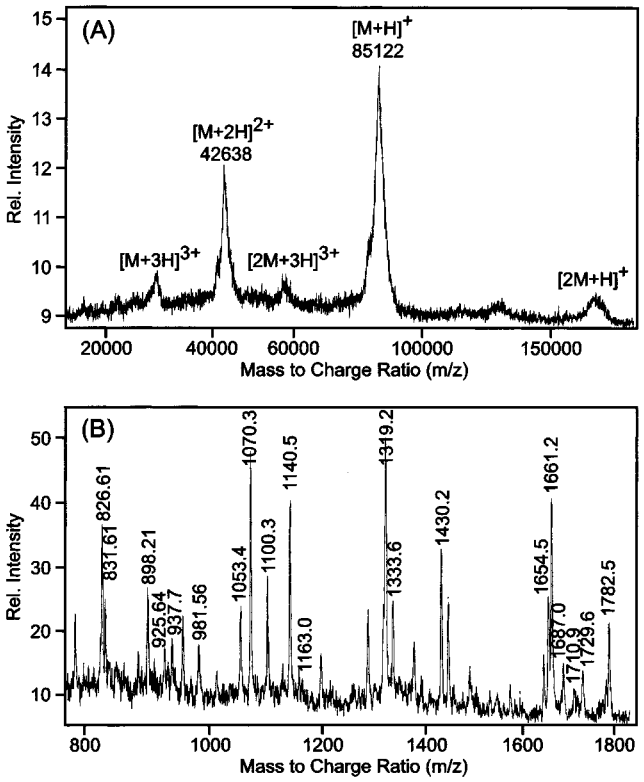

FIGURE 1: (A) MALDI-TOF mass spectrum of recombinant catalase−peroxidase from the cyanobacterium *Synechocystis* PCC 6803. (B) Tryptic peptide mass map of the *Synechocystis* catalase−peroxidase obtained by MALDI-TOF-MS. Indicated masses are peptide signals which correspond to calculated masses using the PeptideMass software and allowing one missed cleavage.

85 122 Da which is very close to the calculated value of 85 137 Da (753 amino acids of the native enzyme and the hexahistidine tag) (Figure 1A). Moreover, we have digested the protein and compared the MALDI-TOF spectrum of peptides from the tryptic digest (Figure 1B) with calculated peptide masses using the PeptideMass software (*27*). Table 1 summarizes the peptide matches and the mass accuracy of these matches (experimental vs calculated peptide mass). If an error of 1 Da was allowed, 20 matches unequivocally indicated the similarity between the recombinant and wild-type proteins.

Catalytic and Spectral Properties. Recombinant KatG exhibited an overwhelming catalase activity. One milligram of purified KatG catalyzed the formation of 940−1030 μmol of O_2/min in contrast to an oxidation rate of 1.5−2.6 μmol of *o*-dianisidine/min. The corresponding turnover numbers were 1330−1460 s^{-1} for catalase activity and 2.1−3.7 s^{-1} for peroxidase activity. The visible absorption spectrum of the enzyme in the resting state exhibited a Soret peak at 406 nm and broad absorption maxima at 500 and 631 nm (Figure 2A, spectrum 1). The A_{406}/A_{280} ratio varied between 0.62 and 0.65. All these results demonstrated high similarities in spectral and kinetic features of both recombinant and wild-type KatG and thus the suitability of the recombinant form for the investigation of its reaction mechanism by stopped-flow spectroscopy.

Compound I Formation. The initial event in the catalytic mechanism of a peroxidase or catalase is a two-electron oxidation of the enzyme by hydrogen peroxide to an intermediate called compound I (reaction 1). With the exception of cytochrome *c* peroxidase (*29*), compound I of peroxidases normally exhibits the same Soret band maximum as the corresponding native peroxidase but with a hypochromicity of about 40−50%. Thus, its formation can be monitored as the absorbance decrease at this wavelength by conventional stopped-flow techniques. With *Synechocystis* KatG, its high catalase activity made it impossible to monitor compound I formation by addition of hydrogen peroxide to the ferric enzyme. Addition of hydrogen peroxide to ferric KatG in a conventional stopped-flow experiment resulted only in very small absorbance changes (Figure 2C). This was consistent with the observation that the dominant steady-state species during hydrogen peroxide degradation exhibited a spectrum similar to that of ferric KatG (not shown), indicating either that the reduction of compound I by hydrogen peroxide (the classical catalase reaction) back to the resting enzyme (reaction 2) was much faster than formation of compound I by H_2O_2 (reaction 1) or that the catalase reaction does not proceed via compound I.

Table 1: Peptide Masses Obtained by Tryptic Digestion of Recombinant *Synechocystis* Catalase−Peroxidase within the Range of 780−1790 Da, Which Differ by No More Than 1 Da, Using MALDI-TOF-MS

mass determined by MALDI-TOF-MS (Da)	calculated peptide mass (Da)	MC[a]	ΔDa
826.61	826.4	0	0.21
831.61	831.4	0	0.21
898.21	898.4	0	0.19
925.64	925.6	1	0.04
937.70	937.5	0	0.2
981.56	981.5	0	0.06
1053.4	1053.5	0	0.1
1070.3	1070.5	0	0.2
1100.3	1100.5	0	0.2
1140.5	1140.6	0	0.1
1163.0	1163.5	0	0.5
1319.2	1319.7	0	0.5
1333.6	1333.7	1	0.1
1430.2	1430.6	0	0.4
1654.5	1654.8	0	0.3
1661.2	1661.8	0	0.6
1687.0	1687.8	1	0.8
1710.9	1710.9	1	0
1729.6	1729.9	0	0.3
1782.5	1781.9	1	0.6

[a] Allowed missed cleavages.

$$\text{KatG} + H_2O_2 \rightarrow \text{compound I} + H_2O \quad (1)$$

$$\text{compound I} + H_2O_2 \rightarrow \text{KatG} + H_2O + O_2 \quad (2)$$

$$\text{compound I} + AH_2 \rightarrow \text{compound II} + AH^{\bullet} \quad (3)$$

$$\text{compound II} + AH_2 \rightarrow \text{KatG} + AH^{\bullet} \quad (4)$$

Consequently, we used peroxoacetic acid to form a stable KatG compound I and to investigate its reactivity. Figure 2A (spectrum 2) shows the spectrum of KatG compound I produced by mixing 20 μM recombinant enzyme with 200 μM peroxoacetic acid. Its spectrum was distinguished from that of the resting state by a 40% hypochromicity at 406 nm and two distinct peaks at 604 and 643 nm. Isosbestic points between compound I and the resting enzyme were determined to be at 357, 430, and 516 nm. A typical time trace for the reaction of peroxoacetic acid with ferric KatG is

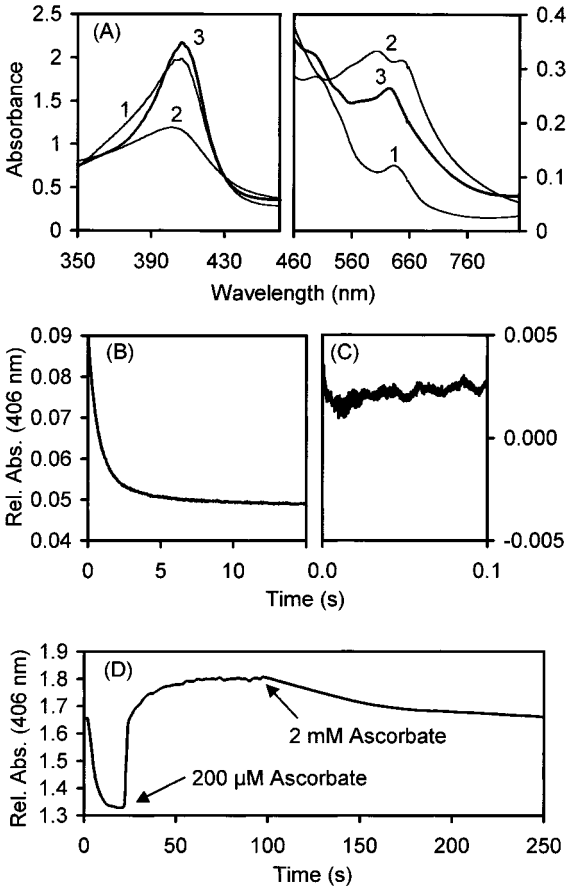

FIGURE 2: (A) Absorption spectra of cyanobacterial catalase−peroxidase and its oxidized intermediates. Spectra of (1) 20 μM native enzyme, (2) compound I produced by mixing 20 μM enzyme with 200 μM peroxoacetic acid and waiting for 20 s, and (3) compound II formed by mixing 20 μM enzyme with 200 μM peroxoacetic acid, after 20 s adding of 200 μM ascorbate, and waiting for 5 s. The spectra were recorded in 50 mM phosphate buffer at pH 7.0 and room temperature. (B and C) Typical stopped-flow time traces of the reaction of ferric KatG (1 μM) with (B) peroxoacetic acid (100 μM) and (C) hydrogen peroxide (20 μM) at 407 nm. Buffer and temperature conditions were like those described for panel A. (D) Consecutive formation of compound I, compound II, and ferric enzyme monitored at 406 nm. Ferric KatG (20 μM) was mixed with peroxoacetic acid (200 μM) at time zero. At 20 s, preformed compound I was mixed with 200 μM ascorbate, followed by addition of 2 mM ascorbate at 100 s. Buffer and temperature conditions were like those described for panel A.

shown in Figure 2B. Single-mixing stopped-flow experiments with compound I formation, using excess peroxoacetic acid, gave single-exponential curves, indicating pseudo-first-order kinetics (not shown). Plots of the first-order rate constants versus peroxoacetic acid concentration were linear with very small intercepts (0.04 ± 0.009 s^{-1}), thus underlining the stability of compound I in the absence of a suitable electron donor. From the slope of the plot, the bimolecular rate constant was calculated to be $(8.74 \pm 0.26) \times 10^3$ M^{-1} s^{-1} at pH 7.0 and 15 °C.

Compound I Reduction. It has been outlined above that, in contrast to other peroxidases (e.g., horseradish peroxidase and ascorbate peroxidase), the two-electron reduction of KatG compound I (reaction 2) by hydrogen peroxide seems to dominate over the peroxidase cycle. The peroxidase cycle involves two one-electron reductions (reactions 3 and 4). With horseradish peroxidase or ascorbate peroxidase, a spectroscopically and kinetically distinct enzyme intermediate (compound II) is formed. To investigate the spectral characteristics of KatG compound II, we used the sequential-mixing technique in combination with a diode-array detector. Interestingly, with all classical one-electron donors at various concentrations (ferrocyanide, ascorbate, phenols, or anilines) added to preformed compound I, the rapid scans showed a very small shift but an increase of absorbance in the Soret region (Figure 2A, spectrum 3). The resulting enzyme intermediate closely resembled the spectrum of the native enzyme with the Soret peak shifted to 407 nm and the maximum in the visible region shifted to 626 nm (Figure 2A, spectrum 3). This intermediate was not a stable end product but could be decomposed to the ferric enzyme by further adding one-electron donors. In the experiment whose results are depicted in Figure 2D, ascorbate was used since it is a poor substrate for KatG (*11*), and thus, the corresponding absorbance changes at 406 nm could be easily followed, an indication of both compound I formation and compound I and compound II reduction.

Consequently, the reaction of KatG compound I with one-electron donors was monitored at 407 nm. Since electronic effects of substituents can be used as a probe of the reaction mechanism of a peroxidase, we investigated the reaction of various substituted phenols and anilines with KatG compound I. In a typical sequential-mixing stopped-flow experiment, we premixed a 50-fold excess of peroxoacetic acid with recombinant KatG in the aging loop and incubated it for 20 s. During this aging time, compound I was formed and, finally, was allowed to react with varying concentrations of electron donors. The inset of Figure 3A shows that the progress of the reaction of compound I with 200 μM aniline exhibited a single-exponential behavior which was typical for all investigated electron donors. Figure 3A shows the dependence of the k_{obs} values from the aniline concentration. The plot was linear and showed an intercept at 7.6 ± 0.9 s^{-1}, indicating that the formed redox intermediate was not stable but also reacted with aniline. From its slope, a bimolecular rate constant of $(2.1 \pm 0.2) \times 10^3$ M^{-1} s^{-1} at pH 7.0 and 15 °C was calculated. Similar plots were obtained for the other electron donors, and the calculated rate constants are summarized in Table 2. The pH dependence for the reaction of compound I with aniline exhibited a relatively sharp maximum at pH 5.0 (Figure 3B).

Hammett Plots. The Hammett equation provides a general description of substituent effects upon reaction rates and equilibria of aromatic molecules (*18*):

$$\log(k_X/k_H) = \rho\sigma \qquad (5)$$

where k_X and k_H represent rate (or equilibrium) constants for reactions of substituted and unsubstituted compounds, respectively, σ is the substituent constant, determined by the nature and position of the substituent, and ρ is the reaction constant, which depends on the features and conditions of the reaction. In Table 2, the Hammett σ values of the investigated substrates are listed along with the rate constants. It can be seen unequivocally that the rate of reduction of KatG compound I is strongly affected by para and meta substituents of both phenols and anilines. The adherence to the Hammett equation suggets that both phenols and anilines

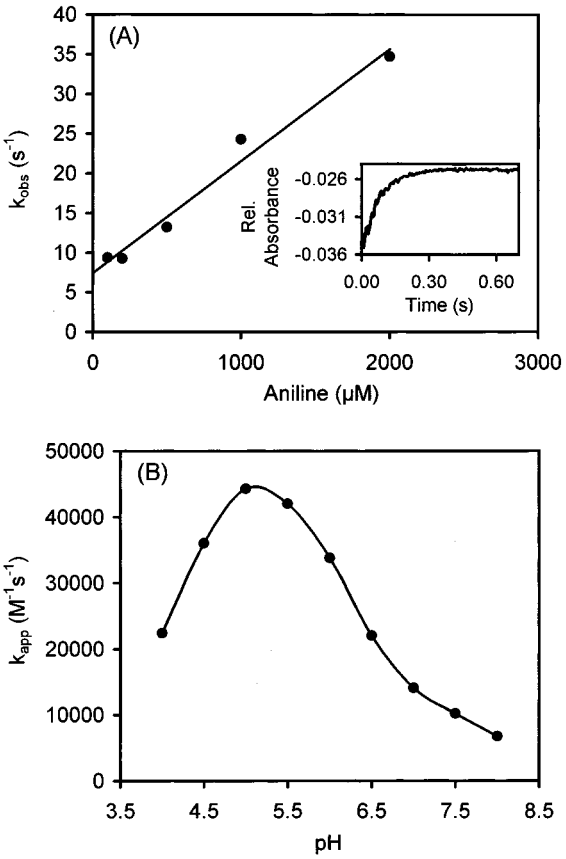

FIGURE 3: (A) Pseudo-first-order rate constants for compound I reduction by aniline at pH 7.0. The inset depicts a typical sequential stopped-flow time trace of the reaction of compound I (1 μM) with aniline (200 μM) monitored at 407 nm. (B) Effect of pH on the second-order rate constants calculated from plots as shown in panel A. The reactions were performed in 50 mM citrate/phosphate buffer at 15 °C.

Table 2: Rate Constants (k_{app}) for the Reduction of Catalase−Peroxidase Compound I with Meta- and Para-Substituted Anilines and Phenols in 50 mM Phosphate Buffer at pH 7.0 and 15 °C and Hammett σ Values of the Aromatic Compounds

aromatic compound	k_{app} (M^{-1} s^{-1})	σ
anilines		
p-hydroxyaniline	$(3.6 \pm 0.1) \times 10^6$	−0.357
p-toluidine	$(9.0 \pm 1.2) \times 10^5$	−0.17
aniline	$(2.1 \pm 0.2) \times 10^4$	0
m-aminobenzoic acid	$(7.0 \pm 0.9) \times 10^2$	0.103
m-aminoacetophenone	$(1.1 \pm 0.3) \times 10^3$	0.306
sulfanilic acid	$(2.1 \pm 0.6) \times 10^3$	0.38
phenols		
p-hydroxyaniline	$(3.6 \pm 0.1) \times 10^6$	−0.66
p-hydroxyanisole	$(3.8 \pm 0.4) \times 10^4$	−0.13
phenol	$(2.3 \pm 0.2) \times 10^3$	0
m-hydroxyanisole	$(5.5 \pm 0.7) \times 10^3$	0.115
p-hydroxybenzenesulfonic acid	$(5.0 \pm 0.1) \times 10^2$	0.38
p-chlorophenol	$(1.1 \pm 0.1) \times 10^4$	0.227

react with compound I via the same mechanism. From the corresponding Hammett plots of $\log(k_X/k_H)$ versus σ (Figures 4 and 5), the value of the susceptibility factor ρ was determined to be -3.4 ± 0.4 for the phenols and -5.1 ± 0.8 for the anilines. The negative slope of the plots indicates that electron-donating groups facilitate oxidation of anilines and phenols. Depending on the nature of the substituent, the rate constants varied by 4 orders of magnitude, e.g., from $(5.0 \pm 0.1) \times 10^2$ M^{-1} s^{-1} for the reaction with *p*-hydroxybenzenesulfonic acid to $(3.6 \pm 0.1) \times 10^6$ M^{-1} s^{-1} for the reaction with *p*-hydroxyaniline.

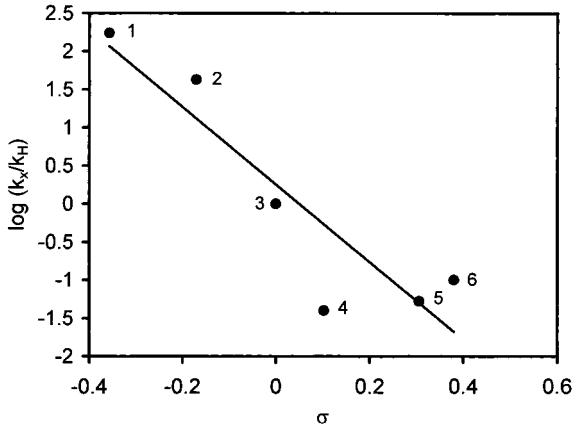

FIGURE 4: Hammett plot of the rate constant of cyanobacterial catalase−peroxidase compound I with meta- and para-substituted anilines at pH 7.0 and 15 °C. k_X is the rate constant for the substituted aniline and k_H for aniline, and σ is the Hammett σ value: (1) *p*-hydroxyaniline, (2) *p*-toluidine, (3) aniline, (4) *m*-aminobenzoic acid, (5) *m*-aminoacetophenone, and (6) sulfanilic acid.

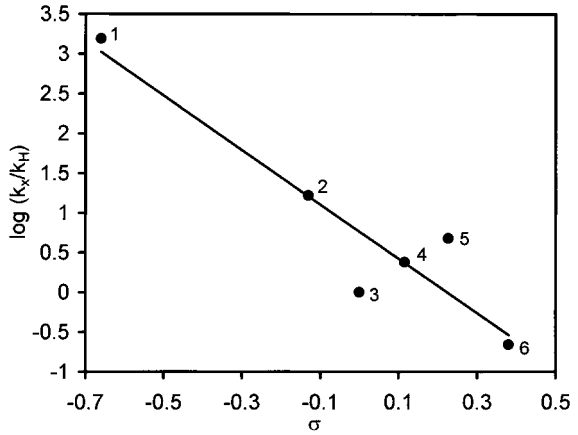

FIGURE 5: Hammett plot of the rate constant of cyanobacterial catalase−peroxidase compound I with meta- and para-substituted phenols at pH 7.0 and 15 °C. k_X is the rate constant for the substituted phenol and k_H for phenol, and σ is the Hammett σ value: (1) *p*-hydroxyaniline, (2) *p*-hydroxyanisole, (3) phenol, (4) *m*-hydroxyanisole, (5) *p*-hydroxybenzenesulfonic acid, and (6) *p*-chlorphenol.

DISCUSSION

Here we describe the design and construction of a system for the high-level production of *Synechocystis* PCC 6803 catalase−peroxidase in *E. coli* and demonstrate its utility for studying the functional properties of this enzyme. Both physical and kinetic properties demonstrated the similarity of the recombinant enzyme and the wild-type protein. Thus, significant quantities of fully intact KatG for the first time permitted comprehensive transient-state kinetic studies of the reaction of the KatG compound I with classical peroxidase substrates. Since there are striking sequence homologies between bifunctional catalase−peroxidases and both ascorbate peroxidases (APXs) and cytochrome *c* peroxidase (CCP) (*2*) but dramatic differences in enzyme reactivities, the kinetic and spectral investigation of enzyme intermediates of catalase−peroxidases is a prerequisite for understanding their bifunctional behavior.

One of the remarkable differences between catalase−peroxidases and both CCP and APX is the high catalase activity of the bacterial enzyme. With CCP and APX, the reaction between the resting enzyme and hydrogen peroxide can be followed by conventional stopped-flow spectroscopy. The transient-state kinetics of compound I formation of pea cytosolic APX revealed second-order rate constants of $8.3 \times 10^7\ M^{-1}\ s^{-1}$ (*29*) and $4.0 \times 10^7\ M^{-1}\ s^{-1}$ (*30*), respectively, and for yeast CCP $10^7-10^8\ M^{-1}\ s^{-1}$ (*31*−*33*). On the contrary, we failed in assessing the formation of KatG compound I because of the high catalase activity (i.e., hydrogen peroxide as the two-electron donor of compound I). Since the enzyme in the ferric form has been shown to be the dominant intermediate during hydrogen peroxide degradation, we assume that the actual rate constant of KatG compound I reduction by hydrogen peroxide exceeds its formation by a factor of at least 5−6. This implies a steady state of 15% compound I or a hypochromicity at the Soret region of about 6%, which fits well with the hypochromicities observed in the reaction of ferric KatG with peroxoacetic acid (Figure 2B) and hydrogen peroxide (Figure 2C). Consequently, we used peroxoacetic acid as a pseudosubstrate of KatG. The utility of alkyl hydroperoxides as pseudosubstrates for monofunctional catalases was first demonstrated by Chance (*34*) and, finally, also the usefulness of peroxoacetic acid in the investigation of the peroxidatic properties of catalase compound I (*35*). KatG compound I, formed with peroxoacetic acid, is remarkably stable, although a very slow regeneration of the spectrum of free KatG occurs. Its spectrum is reminescent of what occurs with plant peroxidases (including ascorbate peroxidases) that form porphyrin π-cation radicals in combination with an iron(IV) center (*36*).

Upon addition of aromatic molecules, the decay of compound I exhibited a typical single-exponential behavior and was strongly dependent on the electron donor concentration. Since reduction of compound I resulted in an intermediate which was not a stable end product but was converted to ferric KatG (Figure 2D), we conclude that compound I contains two oxidizing equivalents, indicating that, in this respect, KatG is similar to other peroxidases.

KatG compound I is the point of intersection of the peroxidase and the catalase cycle. The following evidence suggests different binding sites for two-electron donors (e.g., hydrogen peroxide) and one-electron donors (phenols or anilines). In contrast to addition of one-electron donors, addition of hydrogen peroxide to preformed compound I did not result in formation of ferric KatG as should be expected from steady-state experiments of hydrogen peroxide degradation. Apparently, electron donation from hydrogen peroxide seemed to be blocked. There are several possibilities in explaining this behavior. (i) First, the access for hydrogen peroxide is blocked by excess peroxoacetic acid, but the site of reduction by one-electron donors is not affected. It is known from horseradish peroxidase that suicide substrate inhibition results in the addition of organic groups to the δ-meso carbon of the heme and leads to the loss of activity by sterically blocking access of aromatic electron donors to the heme edge (*37*). In addition, the crystal structure of HRP complexed with the inhibitor benzhydroxamic acid shows binding near this exposed heme edge (*38*). And, recently, evidence was presented that indicates that in APX there are even alternate binding sites for different one-electron donors such as ascorbate and aromatic molecules (*29*). (ii) Second, the catalase reaction does not involve compound I, and (iii) third, the observed compound I species actually contains only one oxidizing equivalent. Whereas none of the first two scenarios can be excluded at the moment, both the spectrum of compound I and the spectrum and kinetic behavior of its reduction product compound II rule out the latter possibility.

As can be seen in Figures 4 and 5, Hammett's rule applies for reduction of KatG compound I by monosubstituted phenols and anilines with different substituents in the meta or para positions. The negative slope of the Hammett plots indicates that electron-donating groups facilitate the oxidation of phenols and anilines, suggesting that the removal of one electron from the substrate is the rate-controlling step in the oxidation reaction. The experimental data are better correlated by the Hammett $\rho\sigma$ relationship than by the Brown−Okamato $\rho\sigma^+$ relationship; the correlation coefficients in the Hammett relationship were 0.83 (anilines) and 0.87 (phenols), and less than 0.61 in the Brown−Okamato relationship. This indicates that the loss of one electron from a substrate is accompanied by the simultaneous loss of a proton so that a positive charge at the reaction site is not formed. A mechanism similar to ours has been suggested for horseradish peroxidase and lactoperoxidase by different authors (*39*−*43*). Our data are in agreement with the behavior of phenols and anilines for oxidation by HRP compound I (*39*) and compound II (*40*−*42*). The reaction constant (ρ) in the Hammett equation obtained in this study was -3.4 ± 0.4 for oxidation of phenols and -5.1 ± 0.8 for oxidation of anilines. The corresponding values of HRP compound I reduction have been determined to be −6.92 (phenols) and −7.0 (anilines) (*39*), whereas the substituent susceptibilities of HRP compound II reactions were -4.6 ± 0.5 (phenols) and -6.0 ± 0.7 (anilines) (*40*, *41*). Thus, KatG compound I exhibits a lower reactivity toward aromatic electron donors than HRP compound I and resembles in its reactivity much more HRP compound II than compound I. The difference in the sensitivity of HRP compounds I and II to electron-donating substituents has been explained by Dunford and co-workers in terms of the relative simplicity of the reactions (*40*, *41*), since differences in reactivity could not be ascribed to redox potentials. These are very similar for the two HRP intermediates in the region at pH 7 (*44*).

Since *Synechocystis* KatG compound I and HRP compound I share similar spectral characteristics, it is reasonable to assume the presence of a ferryl oxygen in combination with a porphyrin π-cation radical in both enzyme intermediates. During the oxidation of phenols or anilines by HRP compound I, the electron-deficient porphyrin moiety of compound I acts as the direct target for an electron donated from the substrate, while in the case of the HRP compound II reaction, in addition to the transfer of an electron to iron(IV), two protons are also transferred to the ferryl oxygen forming a water molecule which leaves from the inner coordination sphere of the iron (*41*). Thus, reduction of HRP compound II is a more complex process than reduction of compound I, since it involves bond-breaking and bond-formation steps. Recently, the different reactivities of the two enzyme states have been also described by application of the Marcus equation (*45*), explaining the lower reactivity of HRP compound II with its longer electron-transfer

distance. In the case of reduction of KatG compound I, at the same time as the transfer of an electron the ferryl oxygen bond seems to be cleaved, since the resulting enzyme intermediate did not exhibit the characteristic spectrally distinct peroxidase compound II spectrum which characterizes the presence of a ferryl oxygen species. Thus, we suggest that during KatG compound I reduction both the porphyrin π-cation radical and the iron(IV) are reduced with one electron derived from the substrate and the second from the KatG protein moiety forming a transient amino acid radical. The resulting enzyme intermediate, compound II, is still one oxidizing equivalent above that of the native enzyme and apparently contains an oxidized amino acid residue which is not electronically coupled to the heme. The occurrence of transient protein radicals is known from cytochrome *c* peroxidase compounds I and II (*46*) and from metmyoglobin and hemoglobin compound I (*47*). Since KatG compound I is relatively stable, the free radical migration apparently occurs in a concerted reaction when the bound aromatic substrate donates its electron to the heme edge. The peroxidase cycle is completed when this transient radical is quenched by oxidation of a second donor molecule. Evidence for this mechanism also comes from the observation that in the absence of classical one-electron donors KatG is reversibly inhibited during hydrogen peroxide degradation and that this inhibition is suppressed in the presence of phenols (*11*). Since the reversibly inhibited enzyme preparations exhibited spectral characteristics similar to those of the ferric protein, it is reasonable to assume that during catalase activity a fraction of the enzyme forms this KatG compound II which is outside the catalase cycle and can only be reduced by typical one-electron donors.

The approximately bell-shaped pH dependence of the k_{app} data (Figure 3B) could be ascribed to two ionizations, that of aniline and one at the active site of compound I. Since the pK_{BH^+} of the anilinium ion (protonated aniline) is 4.6, it seems that only the neutral unprotonated amine reacts with compound I. To relate the kinetics to specific groups at the active site, more data are necessary.

In summary, the developed system for expressing large quantities of recombinant catalase−peroxidase enabled us to study the spectral and kinetic features of KatG compound I and its reactivity toward substituted phenols and anilines. The extraordinary spectral characteristics of KatG compound II as well as its chemical nature are being investigated as well as crystallization studies which should help to elucidate structure−function relationships of this less understood type of heme peroxidase.

REFERENCES

1. Welinder, K. G. (1992) *Curr. Opin. Struct. Biol. 2*, 388−393.
2. Welinder, K. G. (1991) *Biochim. Biophys. Acta 1080*, 215−220.
3. Finzel, B. C., Poulos, T. L., and Kraut, J. (1984) *J. Biol. Chem. 259*, 13027−13036.
4. Patterson, W. R., and Poulos, T. L. (1995) *Biochemistry 34*, 4331−4341.
5. Youn, H.-D., Yim, Y.-I., Kim, K., Hah, Y. C., and Kang, S.-O. (1995) *J. Biol. Chem. 270*, 13740−13747.
6. Marcinkeviciene, J. A., Magliozzo, R. S., and Blanchard, J. S. (1995) *J. Biol. Chem. 270*, 22290−22295.
7. Mutsuda, M., Ishikawa, T., Takeda, T., and Shigeoka, S. (1996) *Biochem. J. 316*, 251−257.
8. Regelsberger, G., Obinger, C., Zoder, R., Altmann, F., and Peschek, G. A. (1999) *FEMS Microbiol. Lett. 170*, 1−12.
9. Nagy, J. M., Cass, A. E. G., and Brown, K. A. (1997) *J. Biol. Chem. 272*, 31265−31271.
10. Johnsson, K., Froland, W. A., and Schultz, P. G. (1997) *J. Biol. Chem. 272*, 2834−2840.
11. Obinger, C., Regelsberger, G., Pircher, A., Sevcik-Klöckler, A., Strasser, G., and Peschek, G. A. (1999) in *Phototrophic Prokaryotes* (Peschek, G. A., Löffelhardt, W., and Schmetterer, G., Eds.) pp 719−731, Plenum Press, New York.
12. Claiborne, A., and Fridovich, I. (1979) *J. Biol. Chem. 254*, 4245−4252.
13. Loprasert, S., Negoro, S., and Okada, H. (1989) *J. Bacteriol. 171*, 4871−4875.
14. Hochman, A., and Goldberg, I. (1991) *Biochim. Biophys. Acta 1077*, 299−307.
15. Hochman, A., Figueredo, A., and Wall, J. D. (1992) *J. Bacteriol. 174*, 3386−3391.
16. Forkl, H., Vandekerckhove, J., Drews, G., and Tadros, M. H. (1993) *Eur. J. Biochem. 214*, 251−258.
17. Obinger, C., Regelsberger, G., Strasser, G., Burner, U., and Peschek, G. A. (1997) *Biochem. Biophys. Res. Commun. 235*, 545−552.
18. Hammett, L. P. (1940) in *Physical Organic Chemistry*, pp 184−199, McGraw-Hill, New York.
19. Stanier, R. Y., Kunisawa, R., Mandel, M., and Cohen-Bazire, G. (1971) *Bacteriol. Rev. 35*, 171−205.
20. Williams, J. G. K. (1988) *Methods Enzymol. 167*, 766−778.
21. Studier, W., Rosenberg, A. H., Dunn, J. J., and Dubendorff, J. W. (1990) *Methods Enzymol. 185*, 60−89.
22. Sanger, F., Nicklen, S., and Coulson, A. R. (1977) *Proc. Natl. Acad. Sci. U.S.A. 74*, 5463−5467.
23. Laemmli, U. K. (1970) *Nature 227*, 680−685.
24. Beers, R. F., and Sizer, I. W. (1952) *J. Biol. Chem. 195*, 133−137.
25. Nelson, D. P., and Kiesow, L. A. (1972) *Anal. Biochem. 49*, 474−478.
26. Jensen, O. N., Shevchenko, A., and Mann, M. (1997) in *Protein Structure-A Practical Approach* (Creighton, T. E., Ed.) pp 29−57, IRL Press, Oxford, U.K.
27. Wilkins, M. R., Lindskog, I., Gasteiger, E., Bairoch, A., Sanchez, J.-C., Hochstrasser, D. F., and Appel, R. D. (1997) *Electrophoresis 18*, 403−408.
28. Kaneko, T., Sato, S., Kotani, H., Tanaka, A., Asamizu, E., Nakamura, Y., Miyajima, N., Hirosawa, M., Sugiura, M., Sasamoto, S., Kimura, T., Hosouchi, T., Matsuno, A., Muraki, A., Nakazaki, N., Naruo, K., Okumura, S., Shimpo, S., Takeuchi, C., Wada, T., Watanabe, A., Yamada, M., Yasude, M., and Tabata, S. (1996) *DNA Res. 3*, 109−136.
29. Mandelman, D., Jamal, J., and Poulos, T. L. (1998) *Biochemistry 37*, 17610−17617.
30. Marquez, L. A., Quitoriano, M., Zilinskas, B. A., and Dunford, H. B. (1996) *FEBS Lett. 389*, 153−156.
31. Balny, C., Anni, H., and Yonetani, T. (1987) *FEBS Lett. 221*, 349−354.
32. Loo, S., and Ermann, J. E. (1975) *Biochemistry 14*, 3467−3470.
33. Ohlsson, P. I., Yonetani, T., and Wold, S. (1986) *Biochim. Biophys. Acta 874*, 160−166.
34. Chance, B. (1949) *J. Biol. Chem. 180*, 947−954.
35. Jones, P., and Middlemiss, D. N. (1972) *Biochem. J. 130*, 411−415.
36. Patterson, W. R., Poulos, T. L., and Goodin, D. B. (1995) *Biochemistry 34*, 4342−4345.
37. Ator, M. A., David, S. K., and Ortiz de Montellano, P. R. (1987) *J. Biol. Chem. 262*, 14954−14960.
38. Henriksen, A., Schuller, D. J., Meno, K., Welinder, K. G., Smith, A. T., and Gajhede, M. (1998) *Biochemistry 37*, 8054−8060.
39. Job, D., and Dunford, H. B. (1976) *Eur. J. Biochem. 66*, 607−614.
40. Dunford, H. B., and Adeneriran, A. J. (1986) *Arch. Biochem. Biophys. 251*, 536−542.

41. Huang, J., and Dunford, H. B. (1990) *Can. J. Chem. 68*, 2159−2163.
42. Sakurada, J., Sekiguchi, R., Sato, K., and Hosoya, T. (1990) *Biochemistry 29*, 4093−4098.
43. Zhang, H., and Dunford, H. B. (1993) *Can. J. Chem. 71*, 1990−1993.
44. Hayashi, Y., and Yamazaki, I. (1979) *J. Biol. Chem. 254*, 9101−9106.
45. Folkes, L. K., and Candeias, L. P. (1997) *FEBS Lett. 412*, 305−308.
46. Catalano, C. E., Choe, Y. S., and Ortiz de Montellano, P. R. (1989) *J. Biol. Chem. 264*, 10534−10541.
47. Miller, M. A., Banyopadhyay, D., Mauro, J. M., Traylor, T. G., and Kraut, J. (1992) *Biochemistry 31*, 2789−2797.

BI990886N